Spherical neutron polarimetry of the magnetic structure in $HoNi_2B_2C$: Interplay between magnetic phases and superconductivity

M. Schneider,* O. Zaharko, and U. Gasser
Laboratory for Neutron Scattering, ETH Zürich & Paul Scherrer Institute, 5232 Villigen PSI, Switzerland

A. Kreyssig
Institut für Festkörperphysik, Technische Universität, 01069 Dresden, Germany

P. J. Brown
Institut Laue Langevin, Boîte Postale 156X, F-38042 Grenoble, France

P. C. Canfield
Ames Laboratory, Department of Physics and Astronomy, Iowa State University, Ames, Iowa 50011, USA
(Received 24 May 2006; published 29 September 2006)

Spherical neutron polarimetry has been used to answer open questions about different magnetic phases in $HoNi_2B_2C$, which are important in their interplay with superconductivity. We established that the incommensurate $\mathbf{a}^*$ structure of $\mathbf{k}_3=(0.585\ 0\ 0)$ at 5.4 K in a zero magnetic field is a transverse-amplitude modulated wave with the magnetic moment along the **b** direction of the tetragonal structure. The depolarization of a neutron beam scattered from the $\mathbf{k}_2=(0\ 0\ 0.915)$ reflections reveals a multidomain state but does not allow an unambiguous determination of the spin configuration. Based on present knowledge of borocarbides and other rare-earth systems we give preference to a long-range incommensurate helical structure as the origin of the $\mathbf{k}_2=(0\ 0\ 0.915)$ reflections.

DOI: 10.1103/PhysRevB.74.104426 PACS number(s): 75.30.−m, 74.25.Ha, 74.70.Dd, 61.12.Ex

I. INTRODUCTION

The rare-earth borocarbides RNi_2B_2C (R=Ho, Dy, Er, and Tm) are regarded as unconventional, since long-range magnetic ordering coexists and competes with superconductivity on a common energy scale. The crystal structure of the borocarbides has a body-centered tetragonal Bravais lattice with $I4/mmm$ space-group symmetry and the lattice parameters $a=b\approx 3.51$ Å and $c\approx 10.53$ Å. $HoNi_2B_2C$ is one of the most interesting of the borocarbide superconductors since the relatively high superconducting transition temperature ($T_C \approx 8.5$ K) lies close above the magnetic transition temperature ($T_N \approx 5.3$ K). Therefore, the system is suited to study the delicate interplay between magnetic and electronic degrees of freedom. $HoNi_2B_2C$ shows three types of antiferromagnetic (AF) structures in zero magnetic field in the narrow temperature range of 4.5 to 5.5 K: a commensurate (CM) structure with a propagation vector of $\mathbf{k}_1=(0\ 0\ 1)$, and two incommensurate (ICM) ones with $\mathbf{k}_2=(0\ 0\ 0.915)$ ($\mathbf{c}^*$-structure) and $\mathbf{k}_3=(0.585\ 0\ 0)$ ($\mathbf{a}^*$-structure).[1] The $\mathbf{k}_1$ magnetic structure consists of ferromagnetic planes of the Ho^{3+} ions stacked antiferromagnetically along the **c** direction. At temperatures below 4.5 K only the CM $\mathbf{k}_1$ structure preserves. Since the discovery of the two incommesurate magnetic modulations in the mid 1990s a lively debate is going on concerning these structures and their influence on the near-reentrant behavior of superconductivity.

Based on a high-resolution x-ray and neutron-scattering study, Hill *et al.* suggested for the $\mathbf{k}_2$ structure a **c**-axis spiral modulation associated with two close-wave vectors $\mathbf{q}_1=0.906\mathbf{c}^*$ and $\mathbf{q}_2=0.919\mathbf{c}^*$.[2] Further, it has been proposed that the modulation is not perfectly sinusoidal. Since the first and third harmonic reflections are present, there is a "squaring" of the spiral.[3] Also, the exact type of the $\mathbf{a}^*$ structure still remains unclear.[1] From neutron-diffraction results on powder samples Loewenhaupt *et al.*[4] concluded that the ICM $\mathbf{k}_3$ has an oscillating component of magnetic moments perpendicular to the (**a**,**b**) plane. In contrast, Hill *et al.*[2] suggested that the ICM $\mathbf{k}_3$ has only magnetic moments perpendicular to the **c** axis. Alternatively, the structure could be a transverse-amplitude modulated wave with a propagation vector along $\mathbf{a}^*$ (or $\mathbf{b}^*$).[3] Moreover, it is not yet settled whether all these wave vectors may coexist in the the same volume fraction or if they compete and are locally separated. A magnetoelastic effect in $HoNi_2B_2C$ was reported by Kreyssig *et al.*[5] At low temperatures $T<T_N$ the tetragonal lattice is slightly distorted along the [1 1 0] axis, in which the long-range ordered Ho moments are aligned.

$HoNi_2B_2C$ is a good example of a local moment system that manifests an extreme basal-plane anisotropy at low temperature. Whether the magnetic long-range order is commensurate or incommensurate is the result of a competition between the crystal electric field (CEF)[6] and the Rudermann-Kittel-Kasuya-Yoshida (RKKY) interaction. Since this indirect exchange interaction is mediated by the conduction electrons, the incommensurate magnetic structure depends on details of the electronic structure. This is the reason why the nesting vector $\mathbf{Q}\approx(0.6\ 0\ 0)$ manifests itself as the modulation wave vector of different incommensurate structures found in various RNi_2B_2C compounds.[1] For $HoNi_2B_2C$ a strong correlation between the near-reentrant behavior of superconductivity and the $\mathbf{a}^*$-modulated structure was emphasized by several authors.[7–9] On the other hand, a mean-field calculation of Amici provides a completely different

 ©2006 The American Physical Society

interpretation.[10] According to this theory the dip in the upper-critical-field (H_{C2}) curve of $HoNi_2B_2C$ results from a small but rapid decrease of the effective interaction parameter due to the onset and fast increase of the magnetic-order parameter. In this picture, the $\mathbf{a}^*$ structure plays only a marginal role for the depression of superconductivity. Nevertheless, a direct manifestation of the electron-phonon coupling was observed in the softening of the phonon spectrum in $HoNi_2B_2C$ at the nesting wave vector along the $\mathbf{a}^*$ axis.[11] Altogether, there is evidence that the ICM $\mathbf{k}_3$ structure is most probably connected with Fermi-surface nesting and therefore the relation of this structure to superconductivity still needs to be resolved.

II. EXPERIMENTS AND RESULTS

We performed a spherical neutron polarimetry experiment on the D3 diffractometer with the CRYOPAD II at ILL in Grenoble, France. The study is based on high-quality single crystals of ^{11}B substituted $HoNi_2B_2C$. They were prepared by a high-temperature flux-growth technique described in Ref. 12. The crystal ($5\times5\times1$ mm^3) was mounted inside an ILL-type orange cryostat with the $\mathbf{b}^*$ direction perpendicular to the scattering plane. The measurements were performed with a neutron wavelength of 0.843 Å (Cu_2MnAl monochromator) at temperatures 2–5.3 K. The polarization of the scattered beam was measured by a ^{3}He neutron spin filter. Since the filter polarization decays with time, this decay was monitored by measuring the polarization of the (0 0 4) structural reflection and the appropriate polarization correction was applied. The scattered polarization was measured for three directions of the incident polarization: parallel to the vertical $\mathbf{z}$ direction, along the scattering vector $\mathbf{Q}\|\mathbf{x}$, and in the $\mathbf{y}$ direction, which completes the right-handed Cartesian set. In this coordinate system the magnetic interaction vector $\mathbf{M}_\perp$, being the projection of the Fourier transform of the magnetization $\mathbf{M}(\mathbf{r})$ onto the plane perpendicular to $\mathbf{Q}$, lies in the $(\mathbf{y},\mathbf{z})$ plane. For a detailed description of spherical neutron polarimetry we refer to Ref. 13. The ordered magnetic Ho moment has been obtained from neutron diffraction measurements performed on the powder diffractometer (DMC) (SINQ,PSI).[14]

A. Data analysis

For a pure magnetic reflection, the cross section for Bragg scattering of a beam of neutrons with polarization $\mathbf{P}_i$ is[15,16]

$$\frac{\partial\sigma}{\partial\Omega} = \mathbf{M}_\perp \cdot \mathbf{M}_\perp^* + \mathbf{P}_i \cdot \mathrm{Im}(\mathbf{M}_\perp \times \mathbf{M}_\perp^*) \tag{1}$$

and the final scattered polarization $\mathbf{P}_f$ is

$$\mathbf{P}_f\frac{\partial\sigma}{\partial\mathbf{\Omega}} = -\mathbf{P}_i(\mathbf{M}_\perp \cdot \mathbf{M}_\perp^*) + 2\,\mathrm{Re}[\mathbf{M}_\perp(\mathbf{P}_i \cdot \mathbf{M}_\perp^*)] - 2\,\mathrm{Im}(\mathbf{M}_\perp \times \mathbf{M}_\perp^*). \tag{2}$$

$\mathbf{M}_\perp^*$ denotes the complex conjugate of the magnetic interaction vector $\mathbf{M}_\perp$. For an amplitude modulated wave the magnetic moment on the jth atom of the lth unit cell may be written as

$$\mathbf{S}_{jl} = \mathbf{A}_j \cos(\boldsymbol{\tau}\cdot\mathbf{r}_l + \phi_j) \tag{3}$$

and for a helix or cycloidal magnetic structure

$$\mathbf{S}_{jl} = \mathbf{A}_j \cos(\boldsymbol{\tau}\cdot\mathbf{r}_l + \phi_j) + \mathbf{B}_j \sin(\boldsymbol{\tau}\cdot\mathbf{r}_l + \phi_j), \tag{4}$$

where $\mathbf{A}_j$ and $\mathbf{B}_j$ are perpendicular vectors. They correspond to the magnitude and direction of the major and minor axis of the elliptical envelope of the spin modulation on the jth atom. $\mathbf{r}_l$ is the vector defining the origin of the lth unit cell and $\boldsymbol{\tau}$ the propagation vector of the modulation. The phases of the modulation are given by ϕ_j. By measuring the change in the polarization state of neutrons scattered by the magnetic reflections one can undoubtedly distinguish whether a modulation of the amplitude or a modulation of the direction of the moments constitutes the magnetic structure.

For neutrons scattered by a pure magnetic reflection of collinear structures ($\mathbf{M}_\perp\|\mathbf{M}_\perp^*$) the polarization $\mathbf{P}_f$ is related to the incident polarization $\mathbf{P}_i$, by precession through 180° about $\mathbf{M}_\perp$. In helical structures, where $\mathbf{M}_\perp$ and $\mathbf{M}_\perp^*$ are not parallel, the situation is different. In this case, if the incident polarization $\mathbf{P}_i$ is perpendicular to the scattering vector $\mathbf{Q}$, the polarization is flipped around the magnetic interaction vector $\mathbf{M}_\perp$ and rotated towards $\mathbf{Q}$.[13] In a multidomain sample, both the cross section and the scattered polarization have to be calculated for each magnetic domain and summed up with weights proportional to the domain fraction. The two most common types of domains are configuration (K) and orientation (S) domains.[17] K domains exist whenever the propagation vector $\mathbf{k}$ describing the magnetic structure is not transformed either into itself, or itself plus a reciprocal vector, by all the symmetry operators of the paramagnetic group. When this is the case the operation of the paramagnetic symmetry on $\mathbf{k}$ generates a set of inequivalent vectors, which form the *star* of $\mathbf{k}$. Each vector in the star generates a different configuration (K) domain. The S domains arise when the symmetry of a magnetic structure is lower than the configurational symmetry.

Each magnetic reflection arises from a single K domain, but may have a contribution from more than one S domain. The presence of S domains leads to a depolarization of the scattered beam.

B. ICM a^* structure

Firstly, we examined the magnetic reflections corresponding to the $\mathbf{a}^*$ structure $\mathbf{k}_3=(0.585\ 0\ 0)$.

The results are presented in Table I. The scattered polarization of the $(h\pm\mathbf{k}_3\ 0\ 0)$ reflections is not rotated when the initial polarization is parallel to $\mathbf{z}$ (the $\mathbf{b}^*$ direction), but is reversed when $\mathbf{P}_i$ is parallel to $\mathbf{x}$ ($\mathbf{a}^*$) or $\mathbf{y}$ ($\mathbf{c}^*$). Besides, there is no significant depolarization of the beam in any of the three cases indicating the presence of only one S domain for the studied K domain. This behavior is unique to the situation where the magnetic interaction vector $\mathbf{M}_\perp$ is along $\mathbf{b}^*$; any component of the magnetic moment along the $\mathbf{c}$ direction

TABLE I. Selected polarimetric data for the wave vector $\mathbf{k}_3$ =(0.58 0 0) for $HoNi_2B_2C$. $\mathbf{P}_i$ is the polarization vector of the incident beam. P_{fx}, P_{fy}, and P_{fz} are the components of the polarization vector of the diffracted beam, corrected for the polarizing efficiency of the spin filter.

(*H K L*) *T* (K)	$\mathbf{P}_i$	P_{fx}	P_{fy}	P_{fz}
(−0.585 0 0)	100	−1.016(20)	0.012(15)	0.076(20)
5.34	010	−0.002(16)	−1.042(20)	−0.029(21)
	001	0.117(22)	−0.055(25)	1.019(21)
(−0.415 0 1)	100	−1.025(28)	0.014(22)	0.047(25)
5.34	010	0.006(22)	−1.024(28)	−0.120(22)
	001	0.091(25)	−0.102(21)	1.023(27)
(0.415 0 −5)	100	−0.996(20)	−0.053(22)	−0.026(28)
5.34	010	0.009(21)	−1.021(25)	0.112(21)
	001	−0.031(27)	0.082(21)	1.032(29)

could, therefore, be excluded. The Ho moments must lie in the (**a**,**b**) basal plane and its major component must point in a **b** direction.

The existence of an **a** component can be probed on the ($h\pm\mathbf{k}_3$ 0 l) reflections ($l\neq 0$). The presence of an **a** component should lead to the nonzero off-diagonal components P_{fy} for the incident **z** polarizations and P_{fz} for the incident **y** polarizations. Under a captious view the entries in Table I [for example, (−0.415 0 1)] could be interpreted as a confirmation of a small **a** component. However, since a single observation can be biased by experimental artifacts (errors in sample alignment, polarization correction, instrument adjustment), we performed a least-squares refinement based on 15 different ($h\pm\mathbf{k}_3$ 0 l) reflections. This refinement confirms that the deviation of the magnetic moments from the [0 1 0] direction does not exceed 4.0(4)°. These results unambiguously show that the $\mathbf{a}^*$ structure is the transverse-amplitude modulation of the magnetic moment along **b** (see Fig. 1). This corroborates one of the ICM structures suggested by Goldman *et al.*[3]

C. ICM $\mathbf{c}^*$ structure

Secondly, we examined the magnetic reflections corresponding to the $\mathbf{c}^*$ structure $\mathbf{k}_2$=(0 0 0.915). These reflections appear in reciprocal space very close to the magnetic reflections (h 0 l) (h+l odd) of the commensurate $\mathbf{k}_1$ =(0 0 1) structure. As the spatial resolution was rather poor, the $\mathbf{k}_2$ and $\mathbf{k}_1$ peaks could not be separated. Therefore, we

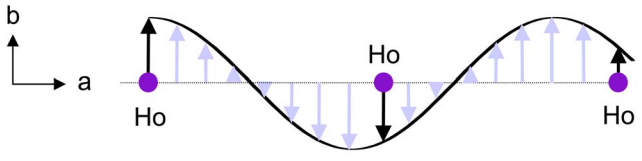

FIG. 1. (Color online) Determined ICM $\mathbf{a}^*$ structure of $HoNi_2B_2C$: amplitude-modulated magnetic moment (**b** direction) propagating in the **a** direction.

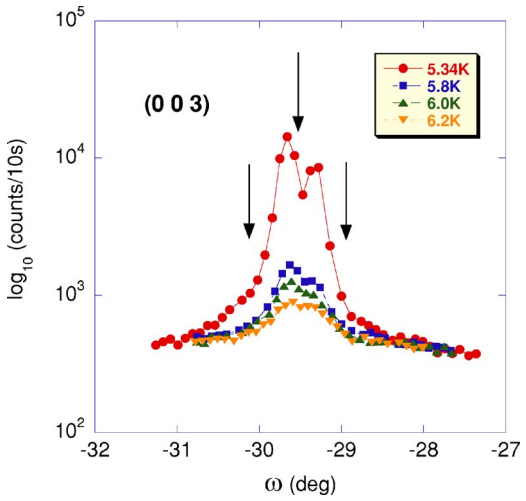

FIG. 2. (Color online) ω scan through the (0 0 3) reflection at several temperatures. Arrows point to the ω values where the polarization analysis has been performed. We attribute the double-peak structure to two slightly twisted crystallites.

analyzed the polarization in the center of the (0 0 3) peak and at the right and left wings at T=5.34 K (see Fig. 2). The scattered polarization is rotated when the initial polarization is parallel to the scattering vector **Q** (Table II) in these three points, therefore, the scattering is purely magnetic. However, the scattered beam is completely depolarized for the P_{iy}, P_{iz} incident polarizations. Due to this depolarization it is not possible to deduce a model of the magnetic structure unambiguously, but the following two classes of models could be proposed:

(1) Long-range $\mathbf{k}_2$ incommensurate magnetic structure with equally populated orientation (S) domains or chiral domains.

(2) $\mathbf{k}_1$ commensurate magnetic structure disturbed by discontinuities appearing regularly at $c/(1-|\mathbf{k}_2|)$.

Figure 3 offers a simplified overview of possible spin arrangements. From the first class of models the transverse-amplitude wave and circular-helix magnetic structure are the simplest cases. The helical (**a**,**b**)-plane spin modulation c_1 in

TABLE II. Polarimetric data for $\mathbf{k}_2$=(0 0 0 0.915) and $\mathbf{k}_1$ =(0 0 1) reflections for $HoNi_2B_2C$. The definition of the symbols is given in Table I.

(*H K L*) *T* (K)	$\mathbf{P}_i$	P_{fx}	P_{fy}	P_{fz}
(0 0 −2.915)	100	−1.027(30)	−0.007(20)	−0.001(20)
5.34	010	0.027(30)	0.017(25)	−0.056(25)
	001	−0.020(25)	−0.065(30)	−0.028(30)
(0 0 −3.0)	100	−1.011(25)	−0.002(20)	−0.012(22)
2.0	010	0.015(21)	−0.026(30)	−0.280(27)
	001	−0.008(22)	−0.280(27)	0.022(25)
(0 0 −3.085)	100	−1.026(30)	0.008(21)	−0.016(25)
5.34	010	0.008(22)	0.015(26)	−0.070(28)
	001	0.002(20)	−0.070(28)	−0.005(22)

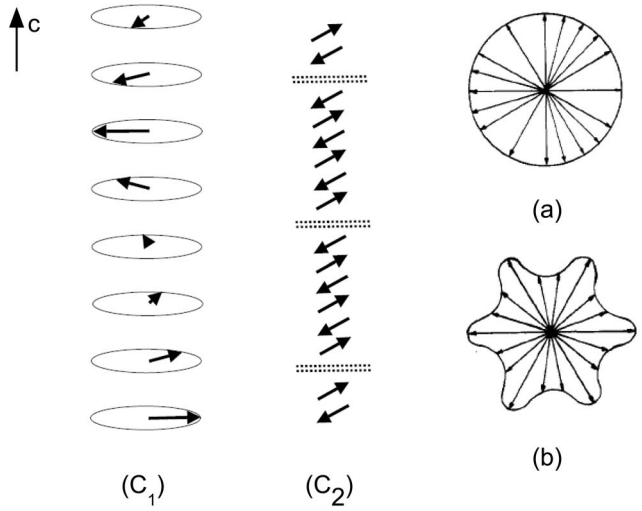

FIG. 3. Two magnetic configurations possible for $HoNi_2B_2C$ with a wave propagating in the **c** direction. (c_1) Helix model. (c_2) Antiphase domain formation with moments in a [1 1 0], respectively, [−1 −1 0] direction. A schematic illustration of Sjöström[20] for two specific magnetic helical structures: (a) bunched circular helix, (b) modulated helix.

Fig. 3 is the most probable model, since the mean-field theory calculations of Amici *et al.* based on this assumption correctly predict the commensurate-to-incommensurate transition in the expected temperature range.[18] Since single-ion CEF anisotropy is significant the structure is most likely more complicated. The anisotropy might not be uniform within the basal plane, being larger for specific directions. This could lead to a bunched helix structure or modulated helix illustrated schematically in Figs. 3(a) and 3(b). Also, a cycloidal modulation cannot be excluded. For the second class of models the presence of disturbances in the long-range collinear $\mathbf{k}_1=(0\ 0\ 1)$ magnetic structure could lead to the appearance of the incommensurate peaks. These disturbances appearing at $c/(1-|\mathbf{k}_2|)\approx 11c$ could be stacking faults, domain walls, defects, or spin slips [see (c_2) in Fig. 3]. From the available data we cannot specify more exactly the origin of such disturbances, but in such a case reflections should be broadened as the disturbances appear not absolutely regular. This is, however, not in agreement with the observations of Hill *et al.*,[2] who reported that the $\mathbf{q}_1$ reflections remain resolution limited, which is indicative of an extremely well-ordered structure, whereas the $\mathbf{q}_2$ modulation has correlation length ξ similar to the CM $\mathbf{k}_1$ structure near the transition temperature ($\xi\approx 600$ Å at $T=5.44$ K). Therefore, we tend to give preference to a long-range helical structure as the origin of the $\mathbf{k}_2$ reflections.

A possible next step to clarify the $\mathbf{k}_2$ magnetic structure would be to apply uniaxial pressure to change the population of the domains in the CRYOPAD experiment.

III. DISCUSSION

Within the statistical accuracy of our experiment, the zero magnetic field ICM $\mathbf{a}^*$ structure of $HoNi_2B_2C$ is a transverse-amplitude modulated wave with the magnetic moments along the **b** direction. We cannot, however, unambiguously determine the $\mathbf{c}^*$ structure from polarimetric data. We give preference to a model of helimagnetic arrangement for the $\mathbf{c}^*$ structure based on the fact that the RKKY exchange, favoring incommensurate helical (or cycloidal) ordering, competes with the single-ion CEF anisotropy, which allows only a limited number of easy magnetic directions. The third harmonics, which we observed in a neutron-diffraction experiment for both ICM $\mathbf{c}^*$ modulations[19] might arise from bunching of the moment directions due to this competition of the RKKY exchange and the CEF anisotropy.[21] Though the presence of regular discontinuities seems to us a less probable reason for the $\mathbf{k}_2$ reflections, it is worth noting that the microstructure plays an important role in $HoNi_2B_2C$: Below, the antiferromagnetic transition crystallographic domains form due to magnetoelastic coupling in order to minimize the free energy. In this context Vinnikov *et al.*[22] reported recently on magnetic flux-line structures (vortices) in the superconducting phase of $HoNi_2B_2C$ caused by pinning at magnetic domain boundaries. The vortex structure of the basal plane consists of stripes along [1 0 0] (respectively, [0 1 0]) with a typical spacing of 1 μm. From the observed linewidth broadening of x-ray-diffraction peaks, Hill *et al.*[2] concluded that in 5.2–5.44 K regime magnetic domains of the CM $\mathbf{k}_1$ structure remain, but the coherence length in the **c** direction is distinctly reduced. Comparing the coherence length obtained by Hill of the short-range ICM $\mathbf{c}^*$ modulation ($\mathbf{q}_2$) with the one they observed for the CM $\mathbf{k}_1$ structure, we tentatively conclude that these two structures coexist in the same domain but that the long-range ICM $\mathbf{c}^*$ modulation ($\mathbf{q}_1$) exists in separate domains. Whether the long-range ICM $\mathbf{a}^*$ modulation exists in distinct domains occupying only part of the crystal or whether this structure is present, superposed on the other modulations throughout the whole volume, remains an open question.

The apparent coexistence of the **a**- and **c**-axis modulations in the (T,H)-phase diagram implies that the two structures have similar free energies and regions of each structure may be stabilized by, e.g., strain, lattice defects, or impurities. In fact, it is also conceivable that the magnetoelastic energy could determine whether the $\mathbf{c}^*$ structure is helical or a spin-density wave, thus stabilizing one of the two states depending on the total energy balance.[10]

The absolute value of the Ho moment cannot be determined reliably from the polarimetric data, therefore we deduced these values based on neutron-powder-diffraction data. Due to the very similar temperature dependence of the ICM structures in both powder and single-crystal samples we believe that such an approach is appropriate. In the refinement we used for the ICM $\mathbf{a}^*$ structure our result from neutron polarimetry, the determined transverse-amplitude modulated wave with the magnetic moments along **b**, and for the ICM $\mathbf{c}^*$ modulation we imposed a helix spin structure with moments restricted to the basal plane.

We performed a FULLPROF refinement (see Fig. 4) assuming the presence of three independent magnetic structures. At $T=5.3$ K the refined value for the ordered moment of the CM $\mathbf{k}_1$ structure was $4.34(3)\mu_B$/Ho, for the ICM $\mathbf{c}^*$ structure $4.09(4)\mu_B$/Ho and for the ICM $\mathbf{a}^*$ structure $3.95(7)\mu_B$/Ho.

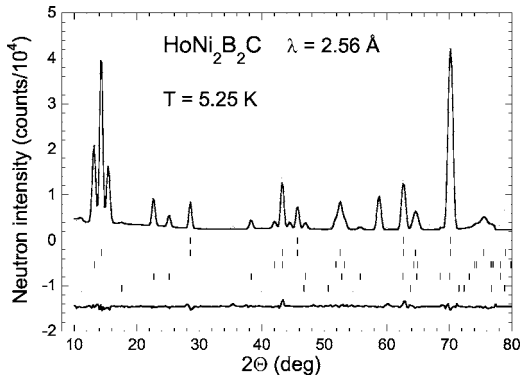

FIG. 4. Neutron powder-diffraction pattern of $HoNi_2B_2C$ at $T=5.25$ K. The first row of the vertical markers denotes the chemical structure, the second row the CM $\mathbf{k}_1$, the third row the ICM $\mathbf{k}_2$, the fourth row the ICM $\mathbf{k}_3$, and the fifth row denotes the third harmonic of the ICM $\mathbf{k}_2$ structure. The regions from 66.5° to 68.5° and from 77.5° to 81.5° with Bragg peaks from the aluminum sample container were excluded from the refinement.

Furthermore, we refined the magnetic moment from powder-diffraction data measured for the antiferromagnetic phase at $T=2$ K. The 2 K-ordered-moment value is $9.06(8)\mu_B$/Ho for the $\mathbf{k}_1$ structure. Based on this, the moments calculated for the $\mathbf{k}_1$, $\mathbf{k}_2$, and $\mathbf{k}_3$ structures at $T=5.3$ K could not belong to the same Ho ion, since the total ordered moment would reach as much as 11.5 μ_B/Ho for certain Ho sites. Even when the third harmonic of the ICM $\mathbf{c}^*$ modulation is included in the calculation (its upper estimate is <1.0 μ_B), the total moment would be 10.5 μ_B/Ho. This estimation provides strong evidence that the magnetic intensity cannot arise from a single magnetic phase with the total moment attributed to one Ho atom, but the moment should be distributed in two or three different types of domains. This is in agreement with the conclusion of Hill *et al.*[2] that the ICM $\mathbf{a}^*$ structure and the ICM $\mathbf{c}^*$ structure do not exist in the same volume of the crystal. Furthermore, the superconductivity of these different domains might be unequal. It is possible that just in one sort of these domains the superconductivity is weakened or even suppressed by the respective magnetic arrangement. We like to underline that the domain formation due to the magnetic order may considerably affect the transport properties (e.g., pinning at the domain walls).

It is worth noting that the onset of the CM $\mathbf{k}_1$ structure is correlated with a pronounced intensity increase of the pure nuclear reflections, e.g., (2 0 0) (see Fig. 5). The intensity variation of nuclear reflections is most probably caused by a change of extinction due to the magnetoelasic effect. By reason of multiple scattering, the strong extinction causes the weakening of the diffracted intensity in perfect crystals of $HoNi_2B_2C$. The formation of the commensurate magnetic

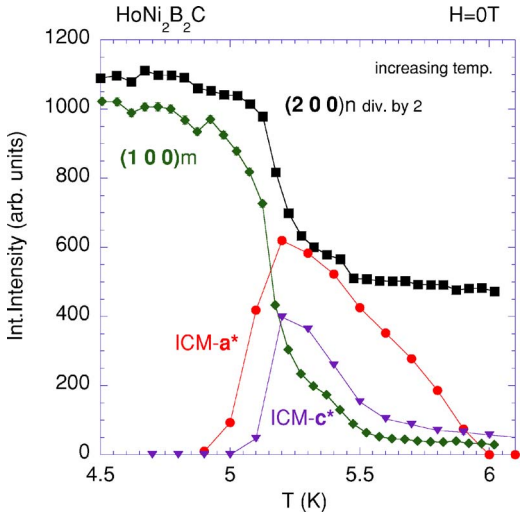

FIG. 5. (Color online) Temperature dependence of three magnetic peaks corresponding to CM $\mathbf{k}_1$ and ICM $\mathbf{k}_2$ and $\mathbf{k}_3$ wave vectors for $HoNi_2B_2C$. The onset of the CM $\mathbf{k}_1$ structure, e.g., (1 0 0) peak is correlated with a pronounced intensity increase of the pure nuclear reflections, e.g., (2 0 0). We ascribe this to a strong extinction effect caused by a pronounced change of domain structure. The solid lines are guides to the eye.

structure leads to a reduction of nuclear-domain size resulting in less multiple scattering and an increase in intensity of the nuclear reflections. Interestingly, the intensity of the nuclear reflections seems not to be affected by the onset of the ICM $\mathbf{a}^*$ modulation. These observations imply that the onset of the $\mathbf{k}_1$ and $\mathbf{k}_2$ structures are associated with a breakdown in crystal perfection, whereas the onset of $\mathbf{k}_3$ is not.

We determined the zero-field ICM $\mathbf{a}^*$ structure, which gives the same order of magnetic intensity as the ICM $\mathbf{c}^*$ structure. The ICM $\mathbf{a}^*$ structure was also observed at a finite magnetic field in $HoNi_2B_2C$ as reported by Detlefs *et al.*,[8] Campbell *et al.*,[23] and Schneider.[19] For an applied external magnetic field in the basal plane the $\mathbf{a}^*$ modulation is even more pronounced in several regions of the (T,H)-phase diagram. Up to now no theoretical model can explain the origin of the $\mathbf{a}^*$ structure. Possibly a more extended description of the RKKY interaction, taking into account the Fermi-surface nesting features[24] is required to improve the theoretical analysis of the interplay between superconductivity and magnetic order in $HoNi_2B_2C$.

ACKNOWLEDGMENTS

We are grateful to N. Kernavanois for expert assistance. This work was partially supported by the Swiss National Science Foundation. A.K. acknowledges financial support by the Deutschen Forschungsgemeinschaft through Grant No. SFB463.

*Electronic address: michael.schneider@psi.ch

[1] K. H. Müller and V. N. Narozhnyi, Rep. Prog. Phys. **64**, 943 (2001).
[2] J. P. Hill, B. J. Sternlieb, D. Gibbs, C. Detlefs, A. I. Goldman, C. Stassis, P. C. Canfield, and B. K. Cho, Phys. Rev. B **53**, 3487 (1996).
[3] A. I. Goldman, C. Stassis, P. C. Canfield, J. Zarestky, P. Dervenagas, B. K. Cho, D. C. Johnston, and B. Sternlieb, Phys. Rev. B **50**, 9668 (1994).
[4] M. Loewenhaupt, A. Kreyssig, C. Sierks, K. H. Mueller, J. Freudenberger, C. Ritter, and H. Schober, ILL Anual Report, 1997 (unpublished).
[5] A. Kreyssig, J. Freudenberger, C. Sierks, M. Loewenhaupt, K. H. Müller, A. Hoser, and N. Stuesser, J. Appl. Phys. **85**, 6058 (1999).
[6] U. Gasser, P. Allenspach, F. Fauth, W. Henggeler, J. Mesot, A. Furrer, S. Rosenkranz, P. Vorderwisch, and M. Buchgeister, Z. Phys. B: Condens. Matter **101**, 345 (1996).
[7] K. H. Müller, A. Kreyssig, A. Handstein, G. Fuchs, C. Ritter, and M. Loewenhaupt, J. Appl. Phys. **81**, 4240 (1997).
[8] C. Detlefs, F. Bourdarot, P. Burlet, P. Dervenagas, S. L. Bud'ko, and P. C. Canfield, Phys. Rev. B **61**, R14916 (2000).
[9] P. C. Canfield and S. L. Bud'ko, in *Rare Earth Transition Metal Borocarbides (Nitrides): Superconducting, Magnetic and Normal State Properties*, NATO Science Series: II. Mathematics, Physics and Chemistry, edited by K. H. Müller and V. Narozhnyi (Kluwer, Dordrecht, 2001), Vol. 14, p. 33.
[10] A. Amici, Ph.D. thesis, Technische Universität Dresden, 1999.
[11] A. Kreyssig, O. Stockert, D. Reznik, F. M. Woodward, J. M. Lynn, W. Reichardt, D. Souptel, G. Behr, and M. Loewenhaupt, Physica B **350**, 69 (2004).
[12] B. K. Cho, P. C. Canfield, L. L. Miller, D. C. Johnston, W. P. Beyermann, and A. Yatskar, Phys. Rev. B **52**, 3684 (1995).
[13] P. J. Brown, J. B. Forsyth, and F. Tasset, Proc. R. Soc. London, Ser. A **442**, 147 (1993).
[14] U. Gasser, Ph.D. thesis, Swiss Federal Institute of Technology, Zurich, 1999.
[15] M. Blume, Phys. Rev. **130**, 1670 (1963).
[16] S. V. Maleev, V. G. Bar'yaktar, and R. A. Suris, Sov. Phys. Solid State **4**, 2533 (1963).
[17] P. J. Brown, Physica B **192**, 14 (1993).
[18] A. Amici and P. Thalmeier, Phys. Rev. B **57**, 10684 (1998).
[19] M. Schneider, Ph.D. thesis, Swiss Federal Institute of Technology, Zurich, 2006.
[20] J. Sjöström, J. Phys.: Condens. Matter **2**, 4637 (1990).
[21] J. Jensen and A. R. Mackintosh, *Rare Earth Magnetism* (Clarendon Press, Oxford, 1991).
[22] L. Ya. Vinnikov, J. Anderegg, S. L. Bud'ko, P. C. Canfield, and V. G. Kogan, Phys. Rev. B **71**, 224513 (2005).
[23] A. J. Campbell, D. McK. Paul, and G. J. McIntyre, Phys. Rev. B **61**, 5872 (2000).
[24] K. H. Müller, J. Freudenberger, G. Fuchs and K. Nenkov, in *Rare Earth Transition Metal Borocarbides (Nitrides): Superconducting, Magnetic and Normal State Properties*, NATO Science Series: II. Mathematics, Physics and Chemistry, edited by K. H. Müller and V. Narozhnyi (Kluwer, Dordrecht, 2001), Vol. 14, p. 255.